Supplemental material for "Ion and Electron Acoustic Bursts during Anti-Parallel Reconnection Driven by Lasers"

Shu Zhang, et al.

February 2022

1 Radiative and non-ideal magnetohydrodynamic simulation using FLASH code for the laser-driven capacitor-coil target

To understand the magnetic field configuration, we have used the radiative and non-ideal magnetohydrodynamic (MHD) FLASH code to simulate the experiment. This simulation is simplified from the 3D geometry an 2D cylindrical geometry, in which the coils are represented by the rings in the planes of the plates. The initial density profile of this simulation is shown in Fig. S1(a). The simulation magnetic field configuration is benchmarked by the proton radiographs measured in the experiments, which is shown in Sec. 2.

The simulation reveals the plasma formed by the laser and the radiation. At $T = 0$, a 1-ns UV laser with 100 μm focal spot is injected along z axis heating the bottom plate of the capacitor. The laser energy is reduced from 3 kJ total energy in the experiment to 2 kJ to compensate the energy loss induced by the laser–plasma instabilities. The radiation from the laser spot also heats the coils and the top plate. The plasmas from the bottom and the top plates collide and squeeze out, generating a plasma flowing toward the coils.

In this FLASH simulation, the magnetic field is advanced based on the induction equation:

$$\frac{\partial \mathbf{B}}{\partial t} = -\nabla \times \mathbf{E}, \tag{1}$$

where

$$\mathbf{E} = \mathbf{u} \times \mathbf{B} + \eta \mathbf{J} + \mathbf{E}_{\text{coil}}, \tag{2}$$

$\mathbf{u}$ is the flow velocity, and $\mathbf{E}_{\text{coil}}$ is the electric field in the coil due to the voltage between the capacitor plates. In the coil region where density $\rho > 1$ g/cm^3, $E_{\text{coil}} = 1.8 \times 10^7$ V/m in azimuthal direction. The corresponding voltage on a

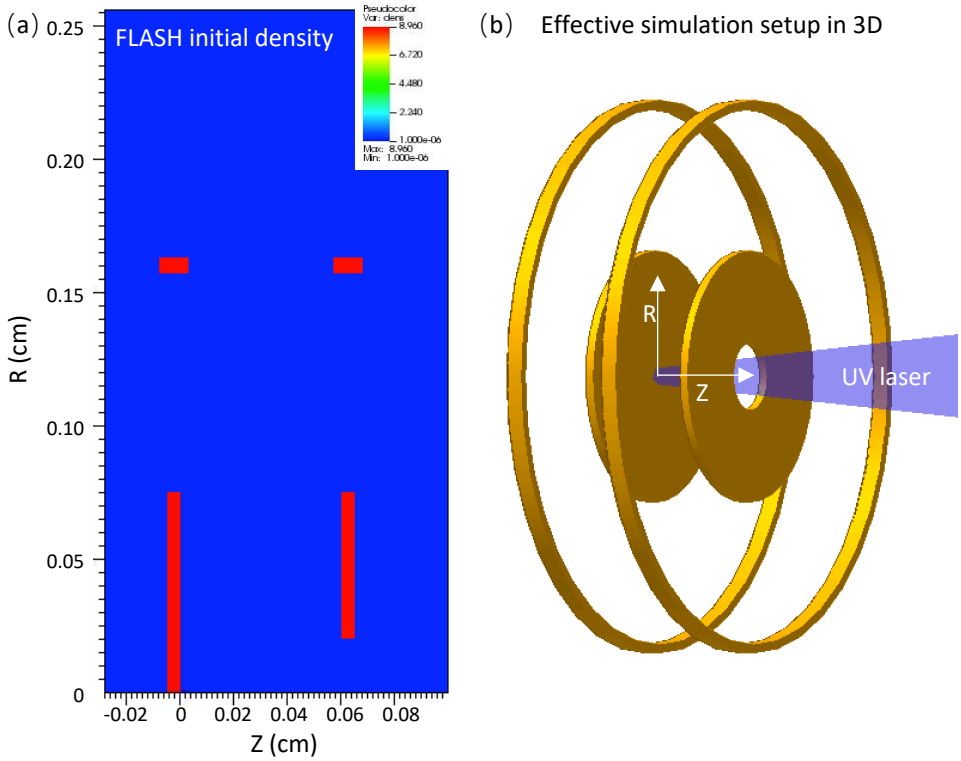

Figure S1: (a) Initial density profile of the FLASH simulation and (b) effective simulation setup in 3D. The two coils are located in at $R = 0.16$ cm and $Z = 0$ and 0.06 cm. Capacitor plates with radius 0.075 cm are center at Z-axis at $Z = 0$ and 0.06 cm. The 1-ns laser beam is along Z-axis. It irradiates the back plate at $Z = 0$ through the entrance hole (200 μm radius) of the front plate at $Z = 0.06$ cm.

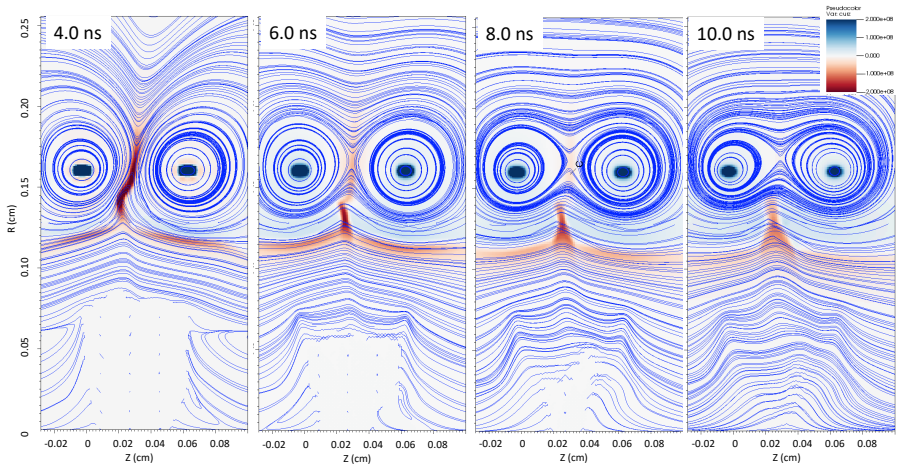

Figure S2: FLASH simulated out of plane current profile overlapped with magnetic field lines (blue lines).

2 mm coil is 36 kV. The resistivity function used in this simulation is

$$\eta = \frac{T_\mathrm{e}}{\frac{5\times10^6}{8\times10^9}\frac{\rho}{8.96} + \frac{T_\mathrm{e}^{5/2}}{8.196\times10^5 \bar{Z}\ln\Lambda} + \frac{3\times10^5}{8\times10^9}\frac{\rho}{8.96}T_\mathrm{e}}. \tag{3}$$

This resistivity is modified from the Al's resistivity model [2],

$$\eta = \frac{1}{5\times10^6 T_\mathrm{e}^{-1} + 170 T_\mathrm{e}^{3/2} + 3\times10^5}\ \Omega\ \mathrm{m}, \tag{4}$$

which is based on the measured Al resistivity from room temperature to 10^6 K [4]. In Eq. (3), η is in FLASH's unit that $\frac{c^2}{4\pi}\eta_\mathrm{Gaussian}=\eta_\mathrm{FLASH}$. The density ρ is in g/cm^{-3}, and the density factor $(\frac{\rho}{8.96})$ is to limit the non-Spitzer resistivity to the high density coil region while keep the low density region as the Spitzer model. The initial coil temperature is set to be 2900 K to reduce numerical instability. However it would cause a higher-than-physical resistivity increasing the current dropping rate. Thus, we choose the duration of the voltage to be 3.5 ns, much longer than the laser pulse length to compensate the higher coil resistivity induced by the high coil initial temperature. The simulated coil current reaches 135 kA at 3.5 ns when the voltage is turned off. Then the current drops exponentially. The coil current is 59 kA at 6.0 ns, which is comparable to the ∼40–70 kA inferred from the proton radiography results.

The simulation suggests that the current sheet is generated by the reconnection between the coils as well as the collision between the plate plasma and the coil plasmas. The current density profile and the magnetic field lines at 4 ns, 6 ns, 8 ns and 10 ns are shown in Fig. S2. Compared with 4 ns, the current sheet in the center breaks into two parts at 6 ns. Then the reconnection current

sheet drops to below 10^7 A/cm^2 at 10 ns, while the collision induced current sheet remains.

The simulated magnetic field has been used to calculate the synthetic proton radiographs and compared with the experimental ones. The synthetic proton radiographs show features similar to the experimental proton radiographs. This benchmark is discussed in Sec. 2.

2 Reconnection features in Proton radiography

In the OMEGA experiment, monoenergetic protons generated by the implosion of a D^3He capsule backlit the capacitor-coil target to diagnose the magnetic field with proton radiography. The D^3He capsule is placed 10 mm in front of the capacitor-coil target, and the CR-39 detectors are placed 25 cm at the back of the target. Proton radiography has also been used in our OMEGA EP experiment with a similar capacitor-coil target as described in Ref. [3, 1], however the protons in OMEGA EP are from Target Normal Sheath Acceleration (TNSA) [5] driven by the 700-fs pulse laser.

As shown in Fig. S3(a), similar to the previous OMEGA EP experiment [1], the OMEGA experiment also shows two voids near the coils and the flask-like feature between the voids. The voids can be reproduced in the synthetic proton radiograph with Biot-Savart-law-calculated 3D B-field profile, as shown in Fig. S3(b,c). They are due to the deflection of protons by the magnetic field around coils.

The flask-like feature can be generated by the pull-reconnection current or the Hall electric field as discussed in Ref. [1]. However, this center feature can also be due to the push reconnection since it can be reproduced with the B-field profile of the FLASH simulation, in which the push-reconnection lasts until 8 ns. Figure S3 (d) and (e) are the synthetic proton radiographs based on the FLASH simulated B-field profile. The center feature is present in the synthetic proton radiographs until 8 ns. However, the void and center feature sizes in the synthetic radiographs have some discrepancies with the measured radiograph. This discrepancy is expected since the simulation has a higher initial coil temperature, which resulted in a faster decay of the coil current and affects the reconnection. In addition, to calculate the synthetic proton radiographs with the 2D simulated B-field, we assume the B-field profile is uniform in a 0.3 mm thick region along the proton beam direction. 3D structure of the B-field in the experiment may affect proton radiography. Also, since the simulation domain is smaller than the measurement, we need to assume no B-field out of the simulation domain.

In addition, even though the center feature can originate from both push and pull reconnection, the measured red-shifted IAW scattering confirmed there is an outflow in the scattering volume, which ruled out the possibility of the pull reconnection.

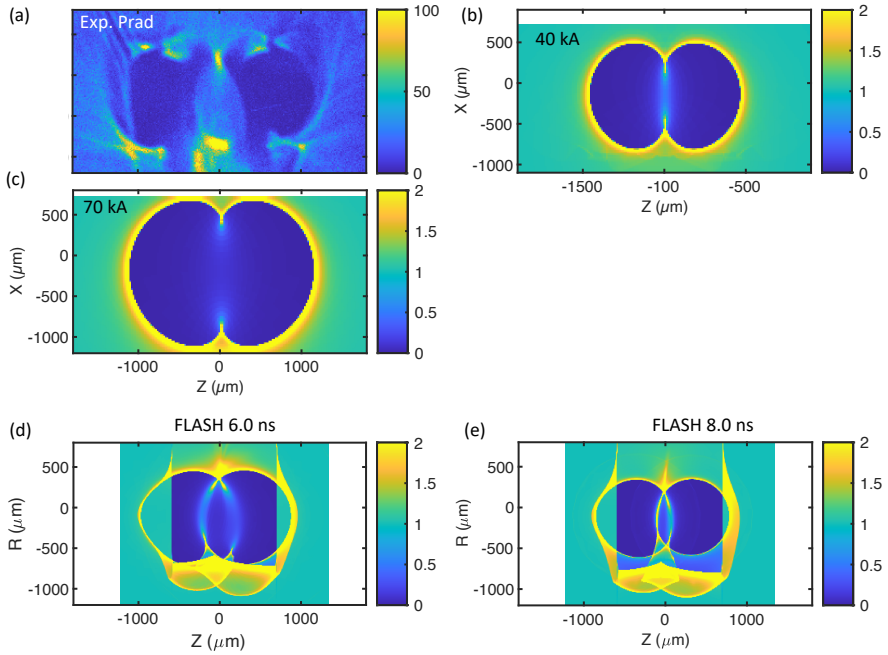

Figure S3: Experimental 15 MeV proton radiograph at 6.0 ns compared with synthetic proton radiographs (b, c, d, e). (b) Synthetic proton radiograph based on the Biot-Savart-law-calculated 3D magnetic profiles with 40 kA coil current. The vertical width of the two voids matches the measured total vertical width. (c) Synthetic proton radiograph with 70 kA coil current. The total horizontal width of the two voids matches the measured total horizontal void width. (d) and (e) are the synthetic proton radiograph based on the FLASH simulated B-field profiles. Both show flask-like center feature similar to the one in the experiment, but the Biot-Savart-law-calcualted proton radiographs did not show this feature. Coordinates in (d) and (e) have been shifted to have the center between coils at $R = 0, Z = 0$. The B-field is filled artificially with 0 in the $|Z| > 600$ μm region out of the FLASH simulation domain, which resulted in uniform proton distribution in that outer region except the caustics deflected the coils.

References

[1] Abraham Chien, Lan Gao, Hantao Ji, Xiaoxia Yuan, Eric G. Blackman, Hui Chen, Philip C. Efthimion, Gennady Fiksel, Dustin H. Froula, Kenneth W. Hill, Kai Huang, Quanming Lu, John D. Moody, and Philip M. Nilson. Study of a magnetically driven reconnection platform using ultrafast proton radiography. *Physics of Plasmas*, 26(6):062113, 2019.

[2] J. R. Davies. How wrong is collisional monte carlo modeling of fast electron transport in high-intensity laser-solid interactions? *Phys. Rev. E*, 65:026407, Jan 2002.

[3] Lan Gao, Hantao Ji, Gennady Fiksel, William Fox, Michelle Evans, and Noel Alfonso. Ultrafast proton radiography of the magnetic fields generated by a laser-driven coil current. *Physics of Plasmas*, 23(4):043106, 2016.

[4] H. M. Milchberg, R. R. Freeman, S. C. Davey, and R. M. More. Resistivity of a simple metal from room temperature to 10^6 k. *Phys. Rev. Lett.*, 61:2364–2367, Nov 1988.

[5] R. A. Snavely, M. H. Key, S. P. Hatchett, T. E. Cowan, M. Roth, T. W. Phillips, M. A. Stoyer, E. A. Henry, T. C. Sangster, M. S. Singh, S. C. Wilks, A. MacKinnon, A. Offenberger, D. M. Pennington, K. Yasuike, A. B. Langdon, B. F. Lasinski, J. Johnson, M. D. Perry, and E. M. Campbell. Intense high-energy proton beams from petawatt-laser irradiation of solids. *Phys. Rev. Lett.*, 85:2945–2948, Oct 2000.